Radio Frequency Performance of DSS 14 64-m Antenna at 3.56- and 1.96-cm Wavelengths

A. J. Freiley
Communications Elements Research Section

During February and March 1973, the DSS 14 64-m antenna was fitted with major structural braces, and other structural modifications were made to improve low angle elevation system gain performance at centimeter wavelengths. The new system performance, as defined by the radiometric measurements of May 1973, is compared to the previous performance, with respect to system efficiency, subreflector focus, and equivalent radio frequency (RF) surface tolerance. The evaluation shows that the predicted effect of the structural braces has been achieved; however, either the main reflector or subreflector surface tolerance, or both, have been degraded. The degradation is well defined at X- and Ku-band frequencies; at S-band the effect is nearly negligible.

I. Introduction

The radio frequency (RF) performance of the DSS 14 64-m antenna was measured to evaluate the effectiveness of the antenna modifications undertaken during February–March 1973. These modifications consisted of the installation of major structural braces and other modifications to the structure for noise abatement (Refs. 1, 2). To obtain the total antenna performance, radiometer measurements of selected radio sources were undertaken at X- and Ku-bands prior to and after the modifications. These radio sources were selected to eliminate the uncertainty associated with less accurately known sources and to maintain consistency with previous measurements. The results show a pronounced change in the antenna RF performance, most likely attributable to a change in antenna surface tolerance.

II. Antenna Modifications

Three major activities occurred during February–March 1973: The first was the installation of the structural braces (Refs. 1, 2) to improve the RF surface tolerance at elevation angles between 6 and 45 deg. Another activity was the resetting of the main reflector panels after the installation of the structural braces. The third activity was the welding of the panels of the subreflector to reduce the noise associated with diplexed high-power microwave transmission.

III. Radio Sources

The performance characteristics were measured using two systems: (1) the X-band system at 8.415 GHz (3.56 cm) and (2) the Ku-band system at 15.3 GHz (1.96 cm). The radiometer measurements were made of 3C123 and Saturn at X-band and Ku-band, respectively. Noise adding radiometers were used at each frequency. Table 1 describes the source characteristics used.

IV. Radiometer Technique

The radiometer technique used consists of three parts: The first is the boresighting of the antenna about the half-power points of the beam. Care was taken to insure both speed and accuracy of the boresights. At these frequencies, the axial focus of the system is important. Therefore, before each set of data was taken, the antenna was focused in the axial direction. To accomplish this, the analog output of the total power noise adding radiometer (NAR) was displayed on a chart recorder. While the antenna beam was on source, the subreflector was slewed from the out position to the in position and back again to determine the optimum indicated position. The third portion of the radiometer technique consists of the on–off source operating system temperature measurements. From two off source and one on source measurements, the off source operating system temperature and the source temperature can be determined for a particular elevation angle. By knowing the flux density of the observed source, one can calculate the antenna efficiency.

V. Radiometer Data

The base performance of the antenna system is defined by measurements made in January 1972 at Ku-band and in January 1973 at X-band. The antenna system performance as determined by the May 1973 measurements is directly comparable. The same sources were observed with the same systems.

The antenna axial focus is an elevation angle dependent function. The fitted curves representing the optimum position for the January X- and Ku-band systems agree very well (Figs. 1, 2). The agreement is within approximately 2.5 mm indicated control room position. The fitted curves representing the optimum position for the May X- and Ku-band systems also agree very well—within approximately 5 mm indicated control room positions. Significant differences occur between the January and the May data. The February–March 1973 modifications have caused the focal length change of the system to become greater as the antenna is moved in elevation. Therefore, the axial focus of the antenna has become more critical for all users.

The off source operating system temperature for clear weather was not affected by the antenna modifications (Fig. 3). The Ku-band operating system temperature is 25 K at zenith, and the X-band operating system temperature is 23 K at zenith, which includes 1.5 K at zenith contributed by the dichroic feed, used during both data periods at X-band (Ref. 3).

The intent of the structural braces was to improve the RF surface tolerance at elevation angles between 6 and 45 deg, which would also improve the RF system efficiency between those angles. The system efficiencies as derived from Table 1 and the radio metric measurements are presented in Figs. 4 and 5. The system efficiencies in the figures are as would be observed in spacecraft and radio science missions; the efficiencies have not been corrected for the atmospheric loss effects (L_0) nor the waveguide loss effects (L_w) but have been corrected for the effect of source size. The results following the structure modifications are lower than expected. The modifications have, in fact, generally decreased the system efficiency, as summarized in Table 2. As shown in Figs. 4 and 5, the modifications have decreased the peak system efficiencies but have improved the change in system efficiency as a function of elevation angle, as was predicted (Ref. 1). The net result is that the peak system efficiency is lower but the system efficiency at 10 deg elevation is about the same as before.

The desirable effect of decreasing the change of system efficiency from the peak was offset by a decrease in the peak system efficiency. To determine a possible cause for the effects seen, one should examine the RF surface tolerance. By assuming a flat-Earth atmospheric loss approximation and using the information given in Table 3 for the calculated system efficiency for 100% efficient reflecting surfaces, and by measuring the actual system efficiency, it is possible to determine the loss due to the surface tolerance. This loss has been converted to an equivalent RMS surface tolerance by the method of Ruze (Ref. 4) and is represented for all cases in Figs. 6 and 7. The RMS surface tolerance of the antenna before the February–March modifications was 1.15 mm at 45 deg elevation, which increased to approximately 1.65 mm at 15 deg elevation. After the modifications, the RMS surface tolerance is approximately 1.46 mm, which increases to 1.62 mm at 15 deg elevation.

VI. Conclusions

The modifications to the DSS 16 64-m antenna accomplished during February–March 1973 have been evaluated at X- and Ku-bands using radiometer techniques. The peak system efficiency at 45 deg elevation angle has decreased at both bands, but the change in system efficiency with elevation angle has been improved.

The conclusions reached are that (1) the structural braces have decreased the effect of the RMS surface tolerance change with elevation angle, and (2) the combination of the main reflector reset and the welding of the subreflector has increased the overall RMS surface tolerance. Another way of stating this is to say that the dynamic distortions (elevation angle dependent gravity induced deformations to the main reflector backup structure) have been improved; the static distortion component (elevation angle independent setting precision of either one or both reflector panels) has been degraded. The reason for the increased axial focus sensitivity as a function of elevation angle is not understood.

The peak system efficiency at 45 deg elevation angle has been reduced 0.5 dB at X-band and 1.6 dB at Ku-band. Using the surface tolerance values obtained from these short-wavelength observations, a predicted change of 0.04 dB at S-band at 45 deg elevation angle is obtained. This loss is reduced at lower elevation angles.

References

1. Katow, M. S., "210-ft-diam Antenna Reflector Upgrade Study–Phase 1," in *The Deep Space Network*, Space Programs Summary 37-62, Vol. II, pp. 109–113, Jet Propulsion Laboratory, Pasadena, Calif., March 31, 1970.
2. Lobb, V. B., and Katow, M. S., "64 Meter-Diameter Antenna with New Braces: Installation Description and Computed Performance for Gravity Loads," in *The Deep Space Network Progress Report*, Technical Report 32-1526, Vol. XVII, pp. 93–99, Jet Propulsion Laboratory, Pasadena, Calif., Oct. 15, 1973.
3. Bathker, D. A., "Dual Frequency Dichroic Feed Performance," presented to the XXVI Meeting of the Avionics Panel, NATO/AGARD, Munich, Germany, November 26–30, 1973.
4. Ruze, J., "Antenna Tolerance Theory–A Review," *Proc. IEEE*, Vol. 54, No. 4, April 1966.

Table 1. Radio sources

Source	S or T_B	Source size, arcsec	Source structure	Antenna half-power beamwidth, arcsec	Antenna polarization
3C123 @ 8.415 GHz	9.4 FU	Two point sources[a]	Close double Sept. 13, arcsec	137	RCP
Saturn @ 15.3 GHz	145 K		Planet (disk)	76	RCP
Jan 72		20 × 18			
May 73		17 × 15			

[a]Source size correction factor (c_s) = 1.003.

Table 2. 64-m system efficiency summary

System	Jan 1973, 45-deg elevation	May 1973 45-deg elevation
X-band	51.3%	46.1%
Ku-band	35.1%[a]	24.1%

[a]January 1972 data.

Table 3. Antenna constants

Constant	X-band	Ku-band
Feed and blockage efficiency η_0 (Ref. 4)	0.6196	0.6411
Waveguide loss L_w, dB	0.14	0.10
Atmospheric attenuation L_0 at zenith, dB	0.037	0.047

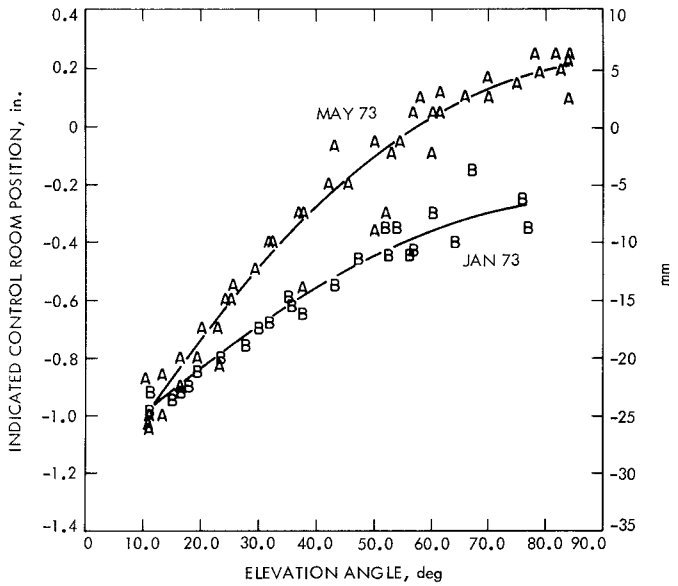

Fig. 1. Axial focus, X-band

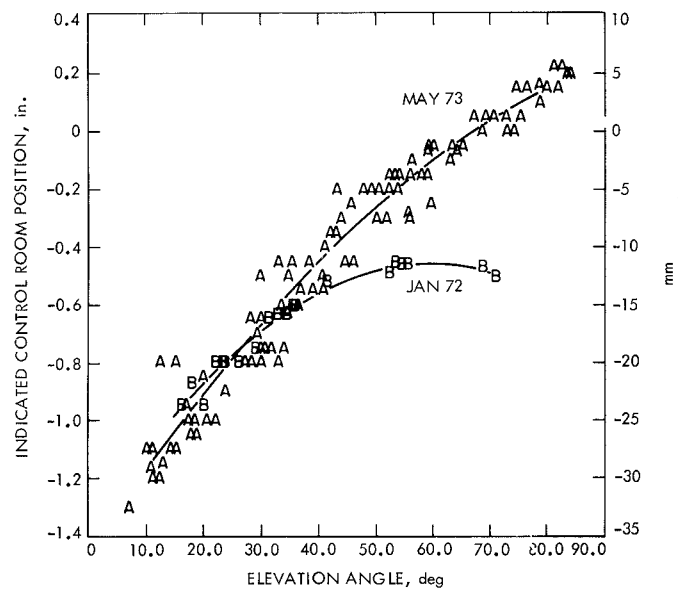

Fig. 2. Axial focus, Ku-band

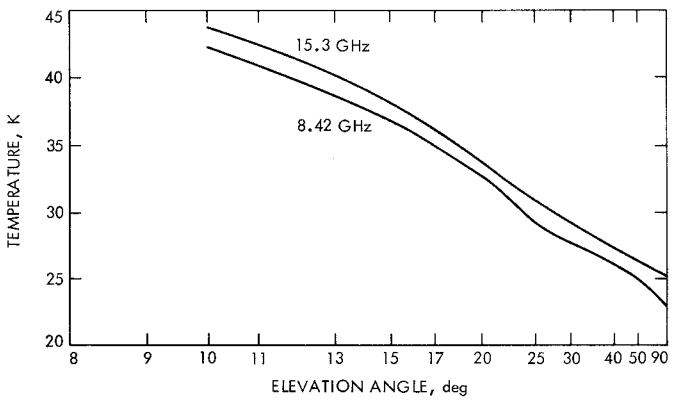

Fig. 3. Operating system temperature

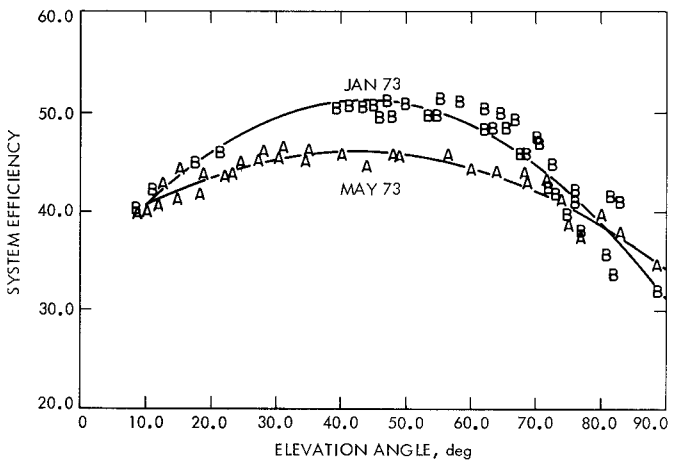

Fig. 4. System efficiencies X-band, 8.42 GHz

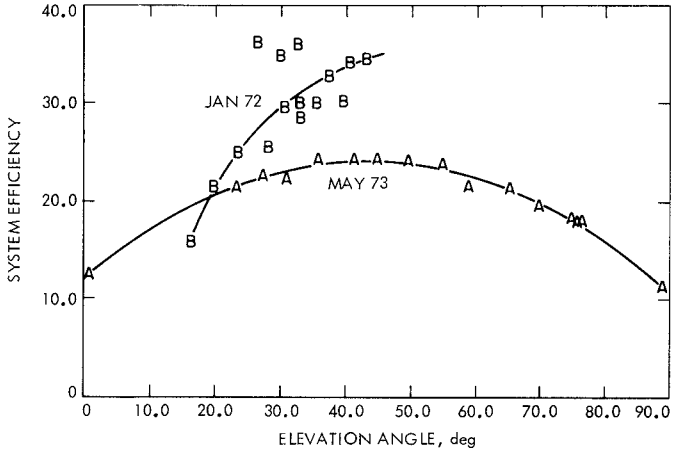

Fig. 5. System efficiencies, Ku-band, 15.3 GHz

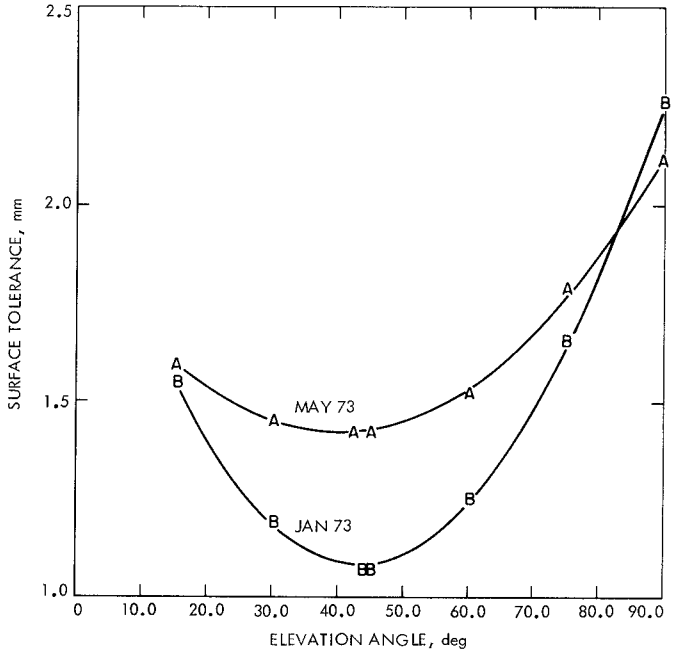

Fig. 6. System surface tolerance from X-band tests

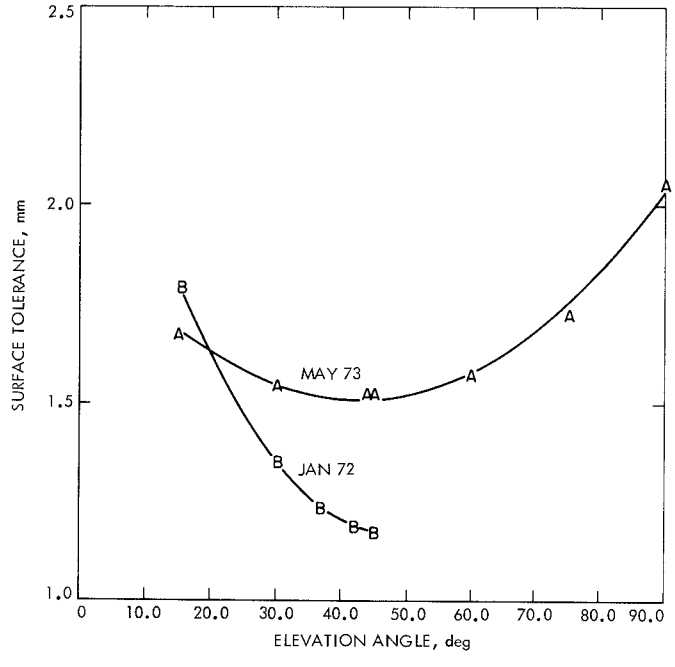

Fig. 7. System surface tolerance from Ku-band tests